2004

Coalescence remnant of spinning binary black holes

J Baker

M. Campanelli

C. O. Lousto

R. Takahashi

Coalescence remnant of spinning binary black holes

J. Baker,[1] M. Campanelli,[2] C. O. Lousto,[2] and R. Takahashi[3]
[1]*Laboratory for High Energy Astrophysics, NASA Goddard Space Flight Center, Greenbelt, Maryland 20771, USA*
[2]*Department of Physics and Astronomy, and Center of Gravitational Wave Astronomy, The University of Texas at Brownsville, Brownsville, Texas 78520, USA*
[3]*Theoretical Astrophysics Center, Dk-2100 København Ø, Denmark*
(Received 13 May 2003; revised manuscript received 6 October 2003; published 30 January 2004)

We compute the gravitational radiation generated in the evolution of a family of close binary black hole configurations, using a combination of numerical and perturbative approximation methods. We evolve the binaries with spins s aligned or counteraligned with the orbital angular momentum from near the innermost stable circular orbit down to the final single rotating black hole. For the moderately spinning holes studied here the remnant Kerr black holes formed at the end of an inspiral process have rotation parameters $a/M \approx 0.72 + 0.32(s/m_H)$, suggesting it is difficult (though not excluded) to end up with near maximally rotating holes from such scenarios.

DOI: 10.1103/PhysRevD.69.027505 PACS number(s): 04.25.Dm, 04.25.Nx, 04.30.Db, 04.70.Bw

I. INTRODUCTION

The coalescence of two black holes of comparable size will provide the most extreme dynamical tests of general relativity's predictions. Such coalescences are an anticipated outcome of galactic collision and core merger. The first galaxy with binary active galactic nuclei has, recently, been discovered by x-ray observations of NGC 6240 with the Chandra Observatory [1]. Possible evidence of merger events has also been recently presented in radio observations of *X*-shaped jet morphologies, which may have been produced by a sudden change in the central black hole's spin axis caused by a supermassive black-hole–black-hole merger [2].

We focus on modeling the final moments of a binary black hole merger, which generates the last few cycles of radiation, carrying away a significant fraction of the system's energy and angular momentum. In a previous paper [3] we have studied nonspinning binary black holes. Our goal here is to extend this treatment to deal with moderately spinning holes focusing, in particular, on the characteristics of the final remnant black hole which the coalescence produces. While we generally expect collisions of binary systems with significant mass ratios, systems with a mass ratio near unity are expected to produce the strongest gravitational radiation (for a given total mass), producing the largest effect on the state of the final black hole. We will restrict to this case here. As we are interested in the dynamics of these systems at their strongest (most nonlinear) moment, we are impelled to apply a model which includes numerical treatment of Einstein's equations in their fully nonlinear form. The results here are thus complementary to previous studies in both the slow-motion weak-field post-Newtonian (PN) approximation, appropriate when the black holes are still far apart [4,5] and extreme mass ratio treatments based on near-geodesic motion [6,7].

In this paper, we adopt the viewpoint that the individual black hole spins vary only slowly as the system approaches the innermost stable circular orbit (ISCO). In general then, we expect pairings of black holes near ISCO with arbitrary spins. We treat the special case of spins either aligned or anti-aligned with the orbital angular momentum, paying particular attention to how this addition of spin to the problem affects the resulting angular momentum of the finally produced black hole. These configurations exclude any precessional effects of the strong field spin interactions, but include the case expected to produce the most rapidly rotating remnant. We apply the Lazarus [3,8–10] approach to treat several systems with moderate spin, allowing us to calculate the radiative loss of energy and angular momentum.

II. THE MODEL

The goal of the Lazarus approach is to exploit a broad range of analytic and numerical techniques to model approximately black hole binaries during the different stages of the coalescence. In particular, while the close limit (CL) approximation Refs. [11,12] can describe appropriately the ring-down of the finally formed black hole, numerical relativity (NR) simulations are needed in order to provide a description of the system in the strong nonlinear merger stage of the collision. We also need a description for the system applicable in the far limit (FL) which can provide initial values for the NR simulations. In this paper we will apply the same CL and NR treatments which we used to study the nonspinning case [3,8–10], but we have extended the FL model to allow spinning black holes.

A. Initial data

We handle spinning black holes in nearly the same way as for the nonspinning case, with the Bowen-York-puncture ansatz [13]. To study plunge radiation we want to begin our simulations with black holes at the innermost stable quasicircular orbit (ISCO) for *spinning* binary black holes as determined for the Bowen-York-puncture initial data. Various approaches have been developed to compute the location and frequency of the ISCO. We will use results based on the effective potential method of [14] as generalized by Pfeiffer, Teukolsky, and Cook [15] for spinning holes. A sequence of quasicircular orbit configurations is determined by minimiz-

TABLE I. Spin - ISCO data based on the effective potential method applied to Bowen-York data.

S	$--0.50$	$--0.37$	$--0.25$	$--0.12$	$++0.00$	$++0.08$	$++0.17$
ℓ/M	7.16	6.80	6.29	5.70	5.05	4.70	4.04
$\pm Y/M$	1.930	1.831	1.651	1.433	1.193	1.062	0.810
$\pm P/M$	0.230	0.236	0.254	0.282	0.326	0.356	0.451
s/M^2	-0.129	-0.0958	-0.0649	-0.0313	0.00	0.021	0.0449
J/M^2	0.629	0.672	0.709	0.747	0.779	0.799	0.820
L/M^2	0.887	0.863	0.838	0.809	0.779	0.757	0.730
$M\Omega$	0.098	0.105	0.118	0.136	0.162	0.182	0.229
m/M	0.424	0.448	0.46	0.464	0.455	0.45	0.435
E_b/M	$-.0159$	$-.0175$	$-.0189$	$-.0208$	$-.023$	$-.0250$	$-.0279$

ing the binding energy with respect to separation along sequences of constant mass ratio, orbital angular momentum and spin. The ISCO is the limit point of this sequence. We also note that the use of Refs. [14,15] results, strictly valid for the ''image method,'' holds for the ''punctures'' since the difference outside the horizons is very small [16] in practice for the fairly detached black holes studied here.

The parameters of seven ISCO orbits are given in Table I. The black holes have parallel spins aligned and counteraligned with the orbital angular momentum as in Ref. [15]. We label the different cases by S, the z-component of each individual black hole's spin, scaled by the square of its horizon mass. This corresponds to the scaled angular momentum parameter a/m for each hole. In the tables, ℓ represents the proper distance between throats, and E_b is the binding energy for the given configuration. Y is the coordinate location of the punctures in conformal space (on the y-axis), P is the linear momentum of the holes (as measured from infinity) and are chosen opposite and transversal to the line joining the holes in conformal space, so that for our simulations the total angular momentum, J, is in the z-direction. We denote by s the individual spin of the holes, and L the orbital angular momentum of the system. The angular frequency of the quasicircular orbit, Ω, is determined from dE_b/dL. Finally, m denotes the individual ''puncture'' (or bare) masses of the holes, and E_b is the binding energy for the given configuration. All quantities are normalized to M, the total ADM mass of the system, and are computed on the initial time slice.

III. RESULTS AND DISCUSSION

In this section we present the results of our simulations beginning from the data described in the last section. As described in Ref. [3], we begin by numerically solving Einstein's equations. The difficulty of performing these numerical simulations limits us to brief evolutions, thus we next apply several criteria in determining when, or whether, the numerical simulation has ''linearized'' and close-limit treatment should be applicable. We first look at the values of the S-invariant [17], which we expect to be within a factor of two of its background value, unity. We also look for independence in the waveforms on the time T when we transition from the numerical simulation to the close limit treatment. In particular, we expect to find independence of the waveform phase over the most significant part of the waveform, as we vary T. We also expect to see some leveling of the dependence of the total radiation energy as we vary T, though this tends to be more difficult to achieve. For each case we will determine waveforms, radiation energy and angular momentum, and the state of the final black hole.

The first configuration we discuss, $SI++0.17$, is the case with the strongest spins aligned with the orbital angular momentum.

In this case we are able to run the numerical simulation long enough to numerically locate a common apparent horizon around the black holes. Figure 1 shows four snapshots of the apparent horizon surfaces [18] on the orbital plane for the $SI++0.17$ case. The dashed line shows the location of

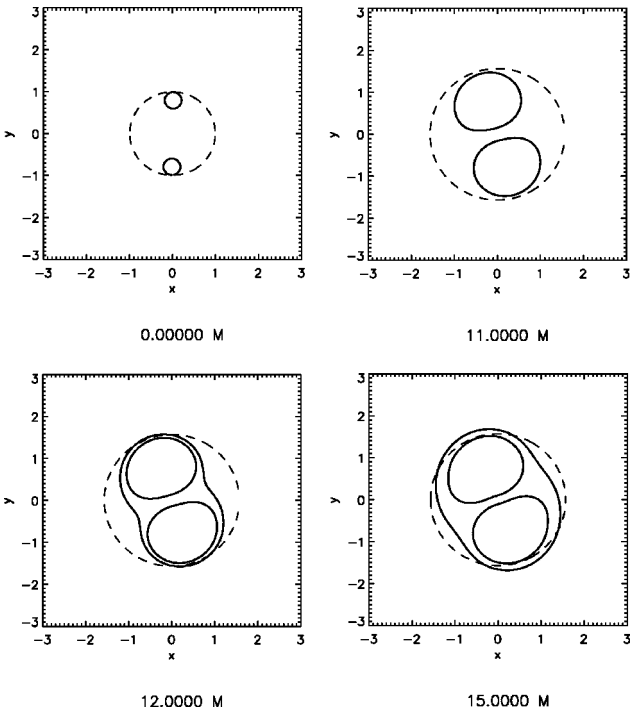

FIG. 1. Horizon formation for $SI++0.17$. The solid curves show the numerically determined location of trapped surfaces including the common apparent horizon of the final black hole. The dashed curve indicates the independently calculated horizon location of the ''background'' perturbed Kerr black hole needed in the CL part of the treatment.

TABLE II. Summary of results for spinning holes.

S	$++0.17$	$++0.08$	$++0.00$	$--0.12$	$--0.25$
T/M	7–9	9–11	9–11	10–12	11–12
$-\Delta E/M(\%)$	1.7–1.9	2.3–2.5	2.4–2.6	1.9–2.1	1.9–2.1
$-\delta J/M^2$	0.06–0.08	0.09–0.10	0.09–0.10	0.09–0.10	0.09–0.10
M_f/M	0.982	0.976	0.975	0.980	0.980
a_f/M_f	0.778	0.739	0.720	0.679	0.639
J_i/M_i^2	0.820	0.799	0.779	0.747	0.709
$M\omega_{peak}$	0.50–0.55	0.45–0.50	0.45–0.50	0.40–0.50	0.40–0.50
$M\omega_{QN}$	0.573	0.552	0.542	0.524	0.508
M/τ_{QN}	0.07714	0.07925	0.08006	0.08160	0.08285
T_{CAH}/M	12	>15	>17	– –	– –

the apparent horizon of the Kerr black hole, which we have identified as the background for the close limit calculation. The plots show that the two black holes are well detached at $T=0$. The ''grid stretching'' effect (due to the vanishing shift we used during full numerical evolution) makes them grow in the coordinate space. These plots are particularly useful to extract qualitative information about the system. Soon after a common apparent horizon covers the system it tends to have an increasingly spherical shape. The time of formation of a common apparent horizon roughly gives an upper limit to the time at which linear theory can take over as has been discussed in Ref. [9]. It is expected that a common *event* horizon should have appeared some M's of time earlier in the evolution of the system. On the independent basis of S-invariant and waveform robustness criteria, we estimate the linearization time to come at $T=7-9M$. This is consistent with the early formation of an apparent horizon. The key physical feature which actually makes the close limit approximation effective is that the black holes share a common potential barrier which appears even earlier than the common event horizon. Near the time of linearization we estimate the location ''background horizon'' at $r_H \approx 1.55$ in the numerical coordinates.

Continuing the evolution in the CL treatment, and after two iterations of the background mass and the radiated angular momentum (starting from the initial data values), we estimate the total energy lost to radiation to be 1.7%–1.9% of the system's initial energy. Likewise, $0.06-0.08M^2$ of the initial angular momentum is lost, resulting in a final Kerr black hole formed after the plunge with $M_f \approx 0.982M$ and $a_f/M_f \approx 0.778$.

The attractive nature of the spin orbit coupling makes the $SI++0.17$, with the strongest aligned component of spin angular momentum the highest frequency and closest configuration at ISCO. As we decrease s, we expect the larger separations to require larger linearization times T. This expectation is consistent with our calculations, which indicate a linearization time of $T=9-11M$ for the $SI++0.08$ and $SI++0.00$ cases, and respectively $T=10-12M$ and $T=11-12M$ for the anti-aligned spin cases $SI-0.12$ and $SI-0.25$. The summarized results are shown in Table II. Overall, energy lost to radiation is near 2%, but peaked at the spinless case. Although the interaction time increases as we decrease s, suggesting more energy could be lost here, the mean frequency of the radiation decreases so that the energy is lost at a reduced rate for the anti-aligned spin cases. The decrease in frequency does not affect the rate at which angular momentum can be radiated as dramatically, which seems to result in a nearly flat s-dependence for the total loss of angular momentum. The ranges given in the tables are estimated from self-consistency tests based on comparisons of perturbative and numerical treatments. Our results may also be subject to systematic errors resulting from effects which may have led us to underestimate the linearization time. We would generally expect any such effect to lead to an increased amount of energy and angular momentum radiated, and a reduction in the final a/m. The results are also subject to errors in the initial model representing black holes at ISCO. A more detailed study of the nonspinning case in [3] indicates some insensitivity in the radiation result to the precise location of ISCO, but further dynamical testing of this class of initial data should be carried out as advances in evolution techniques make it possible.

A particularly interesting quantity derived from each of these results is the angular momentum parameter for the final remnant Kerr holes formed as a product of coalescence. The remnant black holes have a larger rotation parameter a/M for the aligned spin cases than for the anti-aligned ones. In Fig. 2 error bars are estimated by taking the absolute maximum and minimum of the observed damped oscillations of the energy and angular momentum radiated versus the transition time. This provides us with a much larger error than self-consistency tests suggest, but might be more representative of the possible systematic errors of our approach.

It is interesting to note here that the rotation parameters of the final Kerr hole a_f/M_f of Table II and Fig. 2 are large, but still far from the maximally rotating hole, suggesting it is hard to generate near maximally rotating single holes after the plunge of two inspiralling holes, when they have moderate individual rotation parameters like the ones studied in this paper. A curve fitting to the values in Fig. 2 gives $J/M^2 \simeq 0.779+0.2566(s/m_H^2)-0.0941(s/m_H^2)^2$ for the initial data and $a/M \sim 0.719+0.324(s/m_H^2)$ for the final Kerr hole, where m_H is the horizon mass of the individual holes and s its individual spin. If we extrapolate the trend linearly

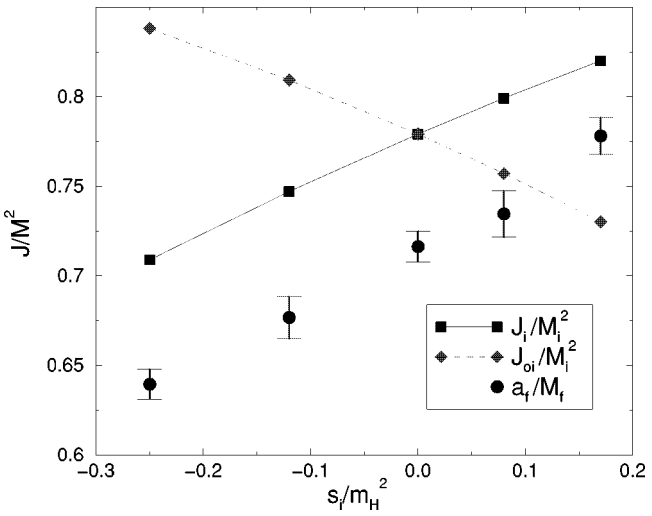

FIG. 2. Rotation parameter for the final remnant Kerr black hole formed by the coalescence of spinning black holes. The plot shows the dependence on the initial individual component of spin aligned with the orbital angular momentum, and normalized to the horizon mass s/m_H^2. The initial orbital and total angular momenta J_o and J_i are also shown.

toward $s/m_H^2 \sim 1$, the result suggests we would require initially aligned holes with spins >0.85 in order to approach a maximally rotating remnant. Our studies thus enhance the conclusions based on complementary studies of binaries in the small mass ratio limit [7] which suggested that it is hard to form a maximally rotating black hole by binary merger unless the mass ratio is near unity. Even in the equal mass case it would seem to take near maximally spinning black holes to produce a maximally spinning remnant. Of course, on a broader astrophysical scenario, rapidly rotating black holes may still be produced by accretion.

We finally note that we also report the binding energy E_b of the initial configurations in Table I for the binary spinning holes. If we interpret this binding energy as a measure of the energy radiated in the form of gravitational waves during the whole inspiral period until we reach the initial configuration we use to estimate the plunge radiation, we come to the notable conclusion that approximately as much energy is radiated in the few cycles following the plunge as in the whole prior lifetime of the binary.

ACKNOWLEDGMENTS

We thank H. Pfeiffer for making available unpublished data related to Ref. [15]. J.B. is supported by the National Research Council. C.O.L and M.C. have financial support from Grants NSF-PHY-0140326 and NASA-URC-Brownsville (NAG5-13396). The full nonlinear numerical simulations have been performed in LRZ (Germany) and NERSC (under Contract No. DE-AC03-76SF00098).

[1] S. Komossa *et al.*, Astrophys. J. Lett. **582**, L15 (2003).
[2] D. Merritt and R.D. Ekers, Science **297**, 1310 (2002).
[3] J. Baker, M. Campanelli, C.O. Lousto, and R. Takahashi, Phys. Rev. D **65**, 124012 (2002).
[4] T. Damour, Phys. Rev. D **64**, 124013 (2001).
[5] L. Blanchet, gr-qc/0201050.
[6] M. Saijo, K.-i. Maeda, M. Shibata, and Y. Mino, Phys. Rev. D **58**, 064005 (1998).
[7] S.A. Hughes and R.D. Blandford, Astrophys. J. Lett. **585**, L101 (2003).
[8] J. Baker, B. Brügmann, M. Campanelli, and C.O. Lousto, Class. Quantum Grav. **17**, L149 (2000).
[9] J. Baker, M. Campanelli, and C.O. Lousto, Phys. Rev. D **65**, 044001 (2002).
[10] J. Baker, B. Brügmann, M. Campanelli, C.O. Lousto, and R. Takahashi, Phys. Rev. Lett. **87**, 121103 (2001).
[11] R.H. Price and J. Pullin, Phys. Rev. Lett. **72**, 3297 (1994).
[12] C.O. Lousto, Phys. Rev. D **63**, 047504 (2001).
[13] S. Brandt and B. Brügmann, Phys. Rev. Lett. **78**, 3606 (1997).
[14] G.B. Cook, Phys. Rev. D **50**, 5025 (1994).
[15] H.P. Pfeiffer, S.A. Teukolsky, and G.B. Cook, Phys. Rev. D **62**, 104018 (2000).
[16] A. Abrahams and R. Price, Phys. Rev. D **53**, 1972 (1996).
[17] J. Baker and M. Campanelli, Phys. Rev. D **62**, 127501 (2000).
[18] M. Alcubierre, S. Brandt, B. Brügmann, C. Gundlach, J. Massó, E. Seidel, and P. Walker, Class. Quantum Grav. **17**, 2159 (2000).